Optimization Design of Bridge Inspection Vehicle Boom Structure based on Improved Genetic Algorithm

Ruihua Xue[1]*, Shuo Lv[2], Tingqi Qiu[3]
Wuhan CCCC Zhuankou Yangtze River Bridge Investment Co., Ltd., Wuhan 430000, China[1, 2]
Chengdu Xinzhu Road & Bridge Machinery Co., Ltd., Chengdu 611400, China[3]

***Abstract*—Excessive self-weight of bridge inspection vehicles increases the safety risk of the inspected bridge structures. In this study, a bridge inspection vehicle arm structure self-weight optimization design model is proposed to improve the efficiency and safety of bridge structure inspection. The model uses a finite element model of the arm structure to generate force data to validate and train a back propagation (BP) neural network-based self-weight prediction model of the arm structure, and uses an improved genetic algorithm to assist the prediction model in searching for the optimal solution. The experimental results show that the maximum stress and maximum deformation of the optimal solution from the optimization model designed in this study are lower than the allowable values of the material, and the total weight of the structure from the optimal solution is the lowest, 4687.5 kg. The computational time of the optimization model designed in this study is lower than all the comparison models. The experimental data show that the optimized model for the self-weight optimization of the bridge inspection vehicle arm structure designed in this study has good optimization effect and has some application potential.**

***Keywords*—Genetic algorithm; Bridge inspection; Structural optimization; Finite element model; BP neural network**

I. Introduction

Currently, the design of mechanical structures in China is generally completed through manpower, specifically relying on the personal experience and professional knowledge of engineers to complete the preliminary design of products [1-3]. This approach highly relies on the personal abilities of the designer, and the design cycle is long, and the design efficiency is also relatively low [4-6]. For large construction machinery such as excavators and bridge inspection vehicles, in most cases, their structural optimization design goal is to minimize the weight of the structure as much as possible while meeting the stress requirements, thereby improving the operational efficiency of the mechanical structure, saving energy and reducing emissions, and reducing construction risks caused by excessive mechanical self-weight [7-9]. As an important part of transport infrastructure, bridges play an irreplaceable role in maintaining traffic safety and ensuring economic development [10-12]. Periodic inspection and maintenance are essential during the operation of bridges [11-13]. As the main equipment for bridge inspection, the design and optimization of the bridge inspection vehicle arm directly affect the effectiveness and efficiency of bridge inspection [14-16]. With the rapid development of artificial intelligence technology represented by neural networks, applying artificial intelligence technology to mechanical structure design has become one of the development trends in mechanical structure design [17-19]. Some previous research has attempted this type of method, but there are still some shortcomings, such as insufficient automation of the designed method and the need to incorporate a certain degree of expert experience into the method. The main reason for this phenomenon is that the parameters in mechanical structure design are complex and numerous, and it is difficult to model using a high level of automation. Therefore, this study attempts to combine finite element model analysis with artificial intelligence algorithms to explore a fast and sufficiently accurate lightweight design method for bridge inspection vehicle arm structures, and uses genetic algorithms to assist in searching for the optimal solution in the optimization model. In addition, considering the inherent drawbacks of genetic algorithms such as being prone to falling into local optima and having poor stability in optimization results, this study innovatively improves the selection operator, mutation, and poor probability calculation methods of genetic algorithms, which is also the importance of this study.

*Corresponding Author.

II. Related Works

Various artificial intelligence algorithms, including BP neural network algorithms, have been applied to a variety of industries and mechanical structure optimization design. Wang D et al. found that the traditional tunnel inspection and reconnaissance methods have high workload and high risk factor. Considering the high mobility of micro-rotor UAV, the authors designed an autonomous tunnel reconnaissance UAV incorporating information from multiple sensors such as inertial measurement units, vision and LIDAR, and used convolutional neural networks to optimize the self-weight of the UAV. The test results show that the optimized UAV reduces its self-weight by 15.7% compared to the pre-optimized UAV, which effectively improves the UAV's endurance [20]. The current additive design capability of Patel D's research team could not meet their production requirements well, so they designed an intelligent additive design system using two neural network architectures, and the test found that the system effectively improved the design efficiency of additive materials [21]. Kien DN et al. constructed a structural defect detection method for mechanical components using Alex neural network and tested that the method resulted in an 8.2% improvement in the accuracy of detecting production defects in mechanical structure design [22]. Li Y et al.

designed a lightweight optimization model for battery structure using radial-based neural network in order to solve the problem of lightweight design of automotive batteries. The experimental results showed that the application of the model reduced the mass of the designed battery pack by 17.62% and the maximum deformation by 30.78% [23]. Fan Y's research team found that the geometry of high-temperature sealed ceramic parts has a significant impact on their compressive resilience performance, so an accurate and large-scale artificial neural network was built to match the relationship between structural parameters and mechanical properties of ZrO_2 parts fabricated through 3D printing. The prediction results show that the combination of artificial neural network and finite element is a better method to optimize the structure and guide the 3D printing method to fabricate complex ceramic parts [24]. Han X et al. proposed a fast, efficient and convenient method to optimize the shape design of centrifugal pump impeller and worm housing by combining genetic algorithm and back propagation neural network. The experimental results showed that the optimized impeller increased the head and efficiency by 7.69% and 4.74%, respectively, at the design flow conditions, while the optimized power was reduced by 2.56%. The hydrostatic pressure across the optimized impeller is more uniform, and the hydraulic performance of the centrifugal pump with the optimized impeller exceeds that of the original centrifugal pump at low and design flow conditions [25]. To AC et al. proposed a new topological optimization method that uses a neural style to simultaneously optimize the mechanical structural performance and geometric similarity of the reference design for a given load condition; this method pre-trains the convolutional layers of the neural network and extracts the geometric similarity. This method also pre-trains the convolutional layers of the neural network and extracts quantitative features from the reference and input data to perform structural optimization. Test results show that the use of this method to optimize the design of mechanical components resulted in the production of components with a 16.7% reduction in dead weight with only a 2.82% increase in maximum stress [26].

In summary, experts in artificial intelligence and mechanical design have conducted extensive research to analyze the possibility and effectiveness of using intelligent algorithms for automatic design of mechanical components. The ideas behind designing these methods may have some inspiration for this study, which is also the connection between this study and previous studies. However, there are still some shortcomings in previous studies, such as insufficient automation of design methods, a certain degree of expert experience still needs to be incorporated into the method. At the same time, the application of this approach to the lightweight design of bridge inspection vehicle structures in previous studies is quite rare. At the same time, the automatic lightweight design of bridge inspection vehicle structures is of great significance in improving the work efficiency of bridge inspection vehicles, saving operating energy consumption, and even reducing the possibility of potential accidents caused by excessive self-weight of inspection vehicles. This is the purpose or objective result of this study. The research may provide some improvement suggestions for the design and manufacturing of future bridge inspection vehicles, which is the impact of this study on the future.

III. Model Design for Weight Optimization of Truss Bridge Inspection Vehicle Arm Structure

A. Finite Element Modeling of the Structure of the Inspection Arm of the Truss-type Bridge Inspection Vehicle

In order to optimize the arm structure of the inspection vehicle, the arm structure needs to be abstracted and modeled first, specifically by establishing its finite element model, in order to remove elements that have no or little influence on the optimization problem and highlight the computational elements that determine the structural optimization results [27]. The loading arm system of truss bridge inspection vehicle consists of gear slewing structure, telescopic working platform, inner and outer working platform, vertical lifting tower and lower slewing truss. The truss bridge inspection vehicle, which is commonly used in bridge construction projects, was selected as the object of this study, and the dimensions of the components to be optimized in its design structure are shown in Fig. 1.

In the optimization problem of truss bridge inspection vehicle arm structure, since the total length of the inner and outer telescopic working platform of the arm truss and the parameters of the lowering depth of the lift tower are determined through the working conditions, it is more reasonable to choose the constructed interface size as a design variable here. Specifically, the sheet thickness and profile dimensions of the interface are selected as design variables. Here, the design variables are first treated as continuous variables to solve the optimization problem, and then the values of the optimal solution are rounded to obtain the appropriate discrete values according to the actual situation. The distribution of design variables of interface dimensions for each type of carriage arm truss rod is shown in Fig. 2.

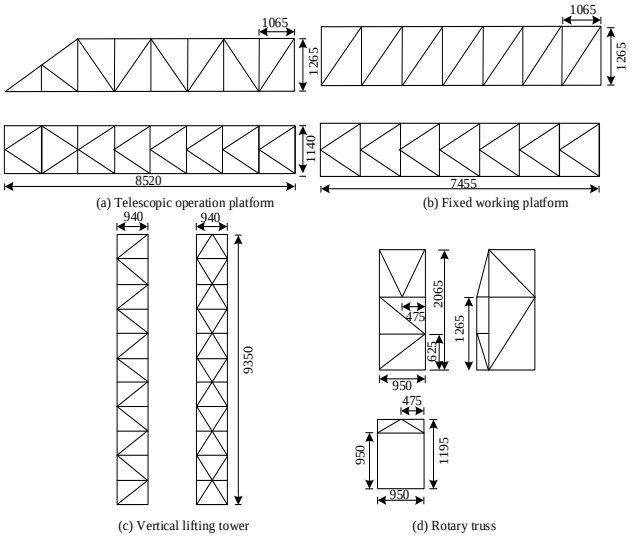

Fig. 1. Common truss bridge inspection vehicle core structure dimensions.

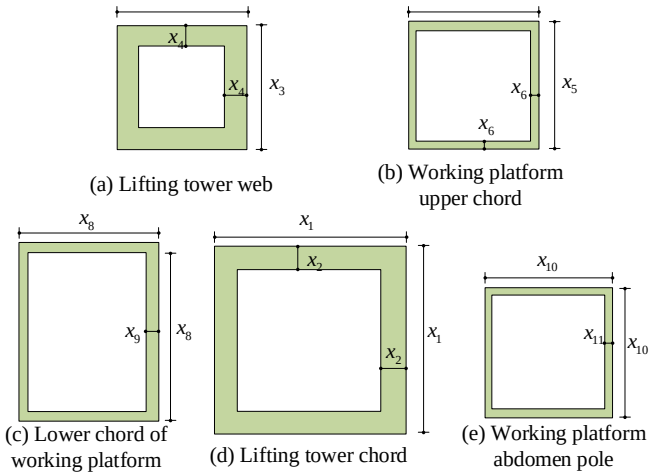

Fig. 2. Distribution of design variables of the arm section of truss bridge inspection vehicle.

The specific meaning of each section design variable, the range of variables, and the initial value of each section design variable of the truss bridge inspection vehicle arm truss in Fig. 2 are shown in Table I. The value range of each variable in Table I is obtained by referring to the corresponding design range of truss bridge inspection truck arm trusses in the industry, and the respective initial values are determined according to the most common values of the same type of products on the market.

TABLE I. DESIGN VARIABLE SPECIFIC INFORMATION DISPLAY TABLE

Parameter number	Variable Symbols	Initial Value	Value range/mm	Variable Meaning
*01	x_1	82	[60,90]	Lifting tower chord cross-sectional dimensions
*02	x_2	11	[5,15]	Cross-sectional material thickness of lift tower stringers
*03	x_3	50	[40,60]	Lifting tower web cross section size
*04	x_4	7	[5,17]	Lifting tower web material thickness
*05	x_5	50	[45,60]	Cross-sectional dimensions of stringers on workbench
*06	x_6	3	[1,8]	Material thickness of stringers on the workbench
*07	x_7	67	[42,75]	Cross-sectional dimensions of the lower chord of the working table
*08	x_8	22	[10,33]	Cross-sectional dimensions of the lower chord of the working table
*09	x_9	5	[2,10]	Material thickness of the lower chord of the working table
*10	x_{10}	45	[25,60]	Cross-sectional dimensions of the lower web of the working table
*11	x_{11}	2.5	[1,8]	Thickness of material of lower web bar of worktable

Considering all kinds of possible working conditions of the inspection vehicle, the most dangerous working condition was selected to carry out the study, i.e. the working condition when the vertical lift tower descends to the lowest position. In this case, the vertical relationship between the telescopic inspection platform and the bridge is vertical, the load borne by the inspection vehicle is 300 M/kg, and the safety factor is 1.5 according to industry regulations.

The parametric model of the truss structure of the inspection vehicle is designed again below. Considering the actual structure of the inspection vehicle arm, it is stipulated that the contact points between the guiding and positioning rollers and the lift tower flange plate are connected by fixed constraints, and the upper and lower end plates of the arm structure are connected by using the gears and bolts of the slewing structure. Although the rotating truss is also connected to the slewing structure and the inner and outer table lap joints using bolts, this part of the modeling is too complex and will significantly increase the number of finite element units and nodes, so the connection structure is ignored and the connection between them is considered as direct coupling. Using the established finite element model to carry out structural statistics and static calculations, it was found that the total mass of the model was 5519.48 kg, and the maximum equivalent stress of the structure was 250.4 MPa, which appeared at the bolt hole of the lower end plate of the rotary structure, while the stress at other locations was much smaller than this value. The strength requirement is satisfied. The maximum displacement of the structure is 98.58mm in the vertical direction of the arm truss, which also meets the structural requirements.

B. Mapping Relationship Model and Mathematical Model Design for Structure Optimization

The computational efficiency of using manual debugging of design variables and then running the finite element model to calculate the optimization target values is particularly low. Therefore, this study uses a BP neural network to construct a mapping relationship between the structural design variables and the optimization objective, i.e., the structural weight of the arm, in order to achieve the goal of fast optimization. The reason for using BP neural network instead of other more complex and advanced neural network algorithms to construct the mapping relationship model is that the target problem in this study is not complicated in terms of features and does not require repeated and high-latitude abstraction extraction, which would substantially increase the computational and training time of the mapping model. And it is difficult to provide a large number of data samples that can make the latter training effective in this study. Before building the mapping model, it is also necessary to select a suitable training sample set. Now, we choose to use the orthogonal test method to obtain the sample data because it generates data samples with neat comparability and balanced distribution, i.e., it is possible to obtain a data set with as complete a distribution as possible with fewer samples. The orthogonal table $L_{50}(5^{11})$ is chosen to obtain the training samples, which contains 5 levels, 50 samples and 11 design factors, as shown in Table II. As shown in Table II, the truss self-weight, maximum deformation and maximum equivalent

force of the model structure are taken as the output in turn, and the required calculation results can be quickly generated by using the finite element model of the inspection vehicle arm.

TABLE II. $L_{50}(5^{11})$ ORTHOGONAL TEST DETAILS

Design Variables	Level 1	Level 2	Level 3	Level 4	Level 5
x_1	81	82	84	85	88
x_2	10	11	12	13	14
x_3	49	51	54	55	57
x_4	8	10	11	12	13
x_5	49	51	55	57	59
x_6	3.0	3.5	4.0	4.5	5.0
x_7	61	62	64	65	68
x_8	21	22	25	27	29
x_9	4.0	4.5	5.0	6.0	6.5
x_{10}	43	44	47	48	51
x_{11}	3.0	3.5	4.0	4.5	5.0

Therefore, the size of the designed BP neural network input data is fixed to 11×50, and the output is the maximum equivalent force and overall mass of the model. Since some of the design variables vary greatly in order of magnitude and may even be out of oversaturation, thus slowing down the convergence or even failing to complete the convergence, the input data need to continue the normalization process. The BP neural network in the mapping model adopts the classical four-layer organization structure, and after several debugging, each layer is substituted with S-type tangent function, S-type logarithmic function, and pure linear function as the transfer function in turn.

The mapping model can be used to quickly calculate the predicted optimization results of the opposing structural solution for the input design variables, but the output value is not the global optimal solution. Therefore, it is also necessary to perform an optimization search operation on the neural network mapping model. The following is a mathematical model of structural optimization required for the optimization search process.

The optimization objective of the mathematical model is to minimize the total weight of the structure while satisfying all the constraints, so as to achieve the effect of improving the efficiency of the drive system and the whole vehicle. Therefore, the objective function and constraints of the structure optimization mathematical model of the detection vehicle are shown in formula (1) and (2), respectively, by calling the three trained BP neural network implicit functions.

$$\min f(x) = sim(net\,G, x) \tag{1}$$

$$\begin{cases} \sigma = sim(net\,S, x) < [\sigma] \\ f = sim(net\ f, x) < [f] \end{cases} \tag{2}$$

In formula (1), $f(x)$ and $net\,G$ are the self-weight function and auto-implicit function of truss respectively, the former is calculated by finite element model and the latter is obtained by BP mapping network training; in formula (2), σ and f are structural stress and vertical displacement respectively, $[\sigma]$ and $[f]$ are allowable stress and allowable stiffness respectively, $net\,S$ and $net\,f$ are structural stress implicit function and vertical maximum displacement implicit function respectively. The input data x satisfy the relationship of formula (3).

$$x \in X = [x_1, x_2, ..., x_{11}]^T \tag{3}$$

C. Design of Optimization Model Solving Method Based on Improved Genetic Algorithm

Genetic algorithm is an optimization algorithm designed after biological genetic rules, which has excellent adaptive ability and large solution set coverage, so it is widely used in solving various complex optimization problems. This time, genetic algorithm is also chosen as the mapping model optimization method, but the traditional genetic algorithm has the following disadvantages. Firstly, the traditional genetic algorithm population initialization is carried out randomly, which may make the mapping model miss the optimal solution, secondly, due to the complex computational content of the mathematical model for structural optimization of the detection vehicle, it will lead to slow convergence of the algorithm, and finally, the traditional genetic algorithm also has the problem that it may fall into local convergence. To alleviate these problems, this study improves the traditional genetic optimization algorithm in many aspects, and the improvement process will be analyzed in detail below.

In the iterative process of genetic algorithm, variation probability and crossover probability play a significant role in the calculation results of the algorithm, and it is necessary to optimize these two parameters because they may even directly lead to the failure of optimization if they are not set properly. In classical genetic algorithms, the variation probability and crossover probability change with the increase of iterations, thus increasing the genetic diversity of the population and reducing the possibility of falling into local optimum. For the classical genetic algorithm, when the fitness of an individual is greater than the average fitness of the population, it means that it is a good individual, and the corresponding variation and crossover probabilities are both a small value, making it easier to save to the next generation. On the contrary, it means that the current individual is a poor adaptor, and its variation and crossover probability are larger values, aiming to improve the quality of its offspring. However, if the individual fitness is equal to the maximum fitness of the population, the corresponding two probability metrics will be reduced to 0. Although this internal regulation model is more reasonable in the later stages of the iteration, when the majority of individuals in the population are excellent and the impact of variation adjustment should be minimized. However, in other stages of the iteration, this approach makes the evolution and convergence process too slow, and this is the optimal individual may not be the global optimum. To address the

drawbacks of this adaptive adjustment, previous work has improved the calculation of the crossover probability p_c and the variance probability p_m, as in formulas (4) and (5).

$$p_c = \begin{cases} p_{c1} - \dfrac{(p_{c1} - p_{c2})(f' - f_{avg})}{f_{\max} - f_{avg}}, f' \geq f_{avg} \\ p_{c1}, f' < f_{avg} \end{cases} \quad (4)$$

$$p_m = \begin{cases} p_{m1} - \dfrac{(p_{m1} - p_{m2})(f_{\max} - f)}{f_{\max} - f_{avg}}, f' \geq f_{avg} \\ p_{m1}, f' < f_{avg} \end{cases} \quad (5)$$

In formulas (4) and (5), p_{c1}, p_{c2}, p_{m1}, and p_{m2} are the parameters to be set, and f', f_{avg}, and $f_{\max}$ represent the fitness values of the individuals to be mutated, the average fitness of the population, and the maximum fitness, respectively. This improved calculation method uses an elite retention strategy, which protects the best individuals in each generation. However, the parameter of the number of iterations of the population needs to be added to ensure that the two probabilities will change dynamically, so this study adjusts the calculation of the crossover probability and the variation probability to formulas (6) and (7).

$$p_c = \begin{cases} p_{c1}\left(1 - \cos^2\left(\dfrac{f' - f_{avg}}{f_{\max} - f_{avg} + \lambda} - 1 - \dfrac{\pi}{2}\right)\right), f' \geq f_{avg} \\ p_{c1}, f' < f_{avg} \end{cases} \quad (1)$$

$$p_m = \begin{cases} \dfrac{1}{\sqrt{n}} p_{m1} - \left(1 - \cos^2\left(\dfrac{f_{\max} - f}{f_{\max} - f_{avg} + \lambda} - 1 - \dfrac{\pi}{2}\right)\right), f' \geq f_{avg} \\ \dfrac{1}{\sqrt{n}} p_{m1}, f' < f_{avg} \end{cases} \quad (2)$$

In formulas (6) and (7) λ is a very small positive number, which is added to prevent the occurrence of a situation in the population where the average fitness is equal to the maximum fitness. n, for the number of iterations, the two probabilities are combined with the number of iterations and the trigonometric function, so that they satisfy both non-zero and changeable with the fitness to avoid the situation of falling into local optimum. The selection operation is an indicator to judge whether an individual can be inherited or not. In the optimization problem of this study, the size of the adaptation degree of the optimized solution is closely related to its total structural weight, which means that when the total structural weight is too large, the corresponding solution should be eliminated. For this characteristic, elite retention and roulette selection methods can be chosen to screen genes. The roulette selection strategy allows individuals with greater fitness to be preferentially selected for inheritance to the next generation, facilitating the process of optimization and iteration, which is more common and will not be repeated here. The elite selection strategy can make the better individuals not be destroyed by the hybridization strategy, so the elite selection strategy is chosen as the selection operator of the algorithm. The specific treatment of the elite selection strategy is that when the best individual appears in the population, it is directly copied to the next generation and the subsequent steps are skipped.

The mutation operation serves to increase the genetic richness of the population and prevent the algorithm from early convergence. For the characteristics of the inspection vehicle arm structure weight optimization problem, the mutation operation was chosen to be carried out in this genetic algorithm using the inversion mutation method. The specific processing method is shown in Fig. 3.

However, the disadvantage of this mutation algorithm is that there is no way to know whether the mutated chromosome is superior to the parent, and if the mutated chromosome becomes worse instead, it will instead increase the possibility of local convergence of the algorithm. To avoid this situation, the validity of this mutation needs to be judged after the inversion mutation operation is finished. Here, we choose to use fitness as an indicator to judge the level of chromosomal excellence of the offspring. If the judgment result shows that the chromosome fitness of the offspring is smaller than that of the parent, the mutation operation is deleted, and the result is accepted on the contrary. The improved genetic algorithm was designed by combining the above improved results, and its computational process is shown in Fig. 4. As shown in Fig. 4, firstly, the mapping model based on BP neural network was input into the algorithm, and then the binary coding method was applied to encode the parameters of the improved genetic algorithm, in which several populations were randomly generated, and the fitness function was used to calculate the genetic probability of each individual. Before carrying out the chromosome crossover mutation operation, it is necessary to retain a few good individuals according to the elite strategy, and then judge whether the current operation is inbred, because if it is inbred, it will bring serious adverse effects to the optimization results. If the judgment result is "yes", reselect the operation object and judge again. If the answer is "no", crossover and mutation operations are performed on all individuals according to formulas (6) and (7) to generate new offspring, and finally determine whether the current population and algorithm parameters meet the stop iteration condition, and if so, stop the iteration and output the optimal individual, i.e., the optimal detection vehicle arm structure optimization scheme, and if not, return to the calculation of genetic probability. Step to continue running the algorithm.

This completes the design of the optimized model for the weight of the arm structure of the truss bridge inspection vehicle.

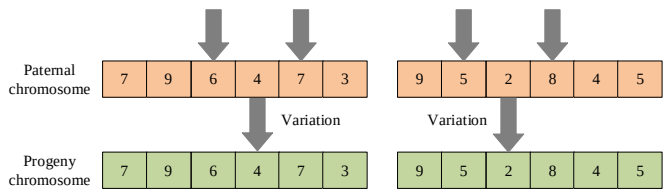

Fig. 3. Schematic diagram of inversion variant treatment.

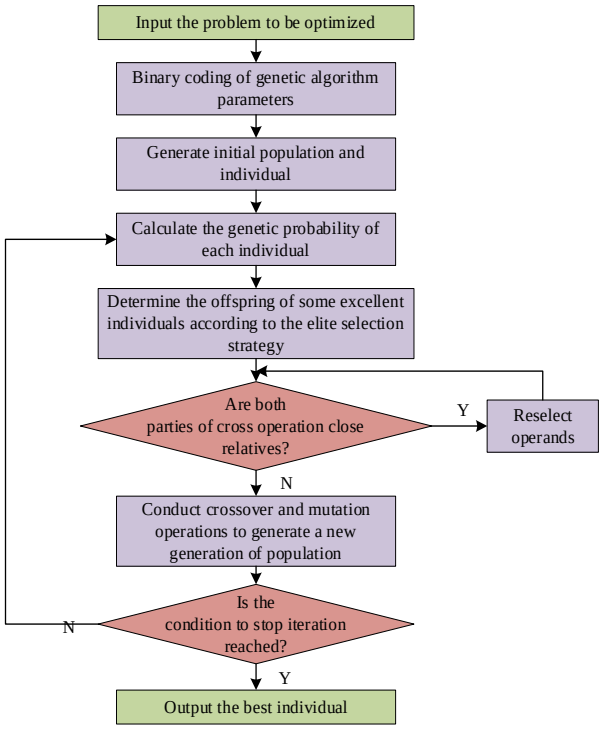

Fig. 4. Flow chart of improved genetic algorithm calculation.

IV. Optimize Model Performance Testing

In order to verify the effect of the optimization method designed in this study on the optimization of the bridge inspection vehicle arm structure, the optimization model designed was implemented using Python language, and its input interface with the finite element model calculation data was built. After several tests and adjustments, the experimental BP neural network model was selected from Trainlm learning method, the maximum number of training steps was fixed to 1000, and the target error was set to 1×10-10. At the same time, the Faster-Regions with CNN features (Faster-RCNN) neural network algorithm, which is widely used in current application scenarios and has excellent performance, was selected to form a comparison model, and finally The following four optimization model schemes are formed: classical genetic algorithm + BP neural network, improved genetic algorithm + BP neural network, classical genetic algorithm + Faster-RCNN neural network, improved genetic algorithm + Faster-RCNN neural network, hereinafter referred to as CGA+BP, IGA+BP, CGA+FRCNN, IGA+FRCNN, respectively.

In order to verify the reasonableness of using neural network algorithm instead of finite element model, after constructing and training the mapping model based on BP and Faster-RCNN, five groups of data different from the training samples were randomly selected to carry out the simulation test, and the test results are shown in Fig. 5. The horizontal axis in Fig. 5 shows each prediction model and the prediction index of the output, the left vertical axis represents the total structural self-weight of the output of various models, and the right vertical axis represents the maximum structural stress of the output of each model. The right vertical axis represents the maximum structural stress output of each model, and the data with percent sign in the figure is the absolute value of the relative error of the output value of the prediction model relative to the output value of the finite element model. As can be seen in Fig. 5, the predicted mean structural dead weight and maximum structural stress of the predictive models based on BP neural network and Faster-RCNN for the five groups of test design variables are 5164.8 kg, 5170.4 kg, 223.63 MPa, 223.95 MPa, and 0.81%, 0.92%, 1.62%, 1.48% respectively. It can be seen that the absolute values of the average relative errors are within the allowed range (less than 5%), indicating that the two selected prediction models can be used. Although the relative error of the structure maximum self-weight prediction value of the Faster-RCNN-based prognostic model is smaller than that of the BP network-based one, the fluctuation of the former prediction is significantly larger, so it is reasonable to select the BP algorithm to construct the prognostic model.

The following analysis of the BP and Faster-RCNN neural network training process in the structural optimization model is shown in Fig. 6. The horizontal axis is the number of model iterations and the vertical axis is the value of the loss function, with different line shapes representing different optimization models. Since the loss function decreases extremely fast in the early stage of model training, the vertical axis is shown in segments. The loss function values after convergence of the two models IGA+BP and IGA+FRCNN constructed using the improved genetic algorithm are significantly lower than those of the other two models, and the former is higher than the latter, at 1.52 and 3.15, respectively, indicating that the global search capability of the algorithm is indeed significantly enhanced after improving the genetic algorithm along the lines of this study. From the perspective of the number of iterations, the model using BP neural network converged significantly faster than the model using Faster-RCNN neural network, for example, IGA+BP and IGA+FRCNN converged after 91 and 169 iterations, respectively.

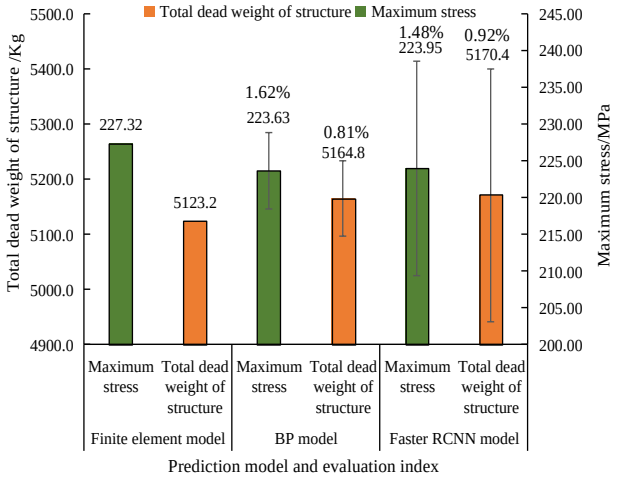

Fig. 5. Comparison of the prediction results of the prediction models.

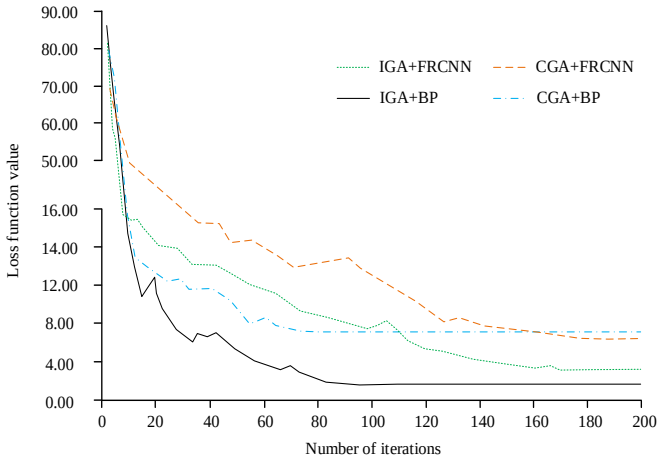

Fig. 6. Comparison of the training process of each optimization model.

In the following, the calculation results of the optimal solution parameters output from each model corresponding to the circular integer value scheme are compared again, as shown in Table III. Observing Table III, it can be seen that after the calculation and processing of each optimization model, some of the design variables of the four optimal integer solutions derived have increased compared to the initial values, but most of the design variables have a significant decrease. From the perspective of maximum stress and maximum deformation, the IGA+FRCNN model is the smallest with 213.9 MPa and 74.64 mm, respectively, followed by the IGA+B0P model with 219.50 MPa and 79.31 mm, respectively. But the maximum stress and maximum deformation of the optimal integer solutions of all the optimized models are smaller than the initial design values and lower than the allowable values. From the perspective of measuring the total structural weight of the measuring arm, the IGA+B0P model has the lowest total structural weight of 4687.5 kg.

Finally, the computational efficiency of each optimization model is analyzed, so different groups of design variables are input and the statistics are obtained in Fig. 7. The horizontal axis in Fig. 7 represents the number of groups of design variables processed by the model consecutively, and the vertical axis represents the total computational time spent. Different curve types represent different optimization models, and the gray vertical lines are auxiliary lines. As can be seen in Fig. 7, the computational time of the model incorporating the FRCNN algorithm is significantly more than that of the model constructed based on the BP algorithm, mainly because the former has a complex structure and more computational levels. Also the computation time of the model using the improved genetic algorithm is significantly lower than that of the model using the same prediction algorithm but without the improved genetic algorithm. For example, when the number of groups of variables with computation is 50, the computation time of each scheme of CGA+BP, IGA+BP, CGA+FRCNN, and IGA+FRCNN is 5.88s, 4.62s, 10.24s, and 9.57s, respectively.

To further compare and study the designed methods, a bridge inspection vehicle optimization method based on incremental algorithm is designed here, and the parameters in the algorithm are determined through multiple debugging methods. The data obtained from the experiment is relatively simple, and it is described in text here. According to the statistical experimental data, it was found that the optimal structural parameters optimized by the IGA+BP model designed in this study still have lower self-weight than the incremental algorithm, indicating that the optimization effect of the latter is worse than that of the former.

TABLE III. COMPARISON OF OPTIMAL INTEGER SOLUTIONS FOR EACH OPTIMIZATION MODEL

Name	Initial design value	CGA+BP	IGA+B0P	CGA+FRCNN	IGA+FRCNN
x_1 /mm	82	74	67	71	69
x_2 /mm	11.00	6.00	6.00	6.00	6.00
x_3 /mm	50	61	58	60	59
x_4 /mm	7.00	7.50	6.50	7.00	6.50
x_5 /mm	50	56	58	58	60
x_6 /mm	3.00	2.50	2.00	2.50	2.50
x_7 /mm	67	52	50	52	50
x_8 /mm	22	16	15	15	16
x_9 /mm	5.00	4.50	4.00	5.00	4.50
x_{10} /mm	45	54	60	62	60
x_{11} /mm	2.50	3.50	4.00	4.00	4.00
Maximum stress/MPa	250.48	227.1	219.50	224.8	213.9
Maximum deformation/ mm	101.36	96.49	79.31	87.15	74.64
Self-weight/ kg	5574.2	5271. 0	4687.5	5188.3	4962.3

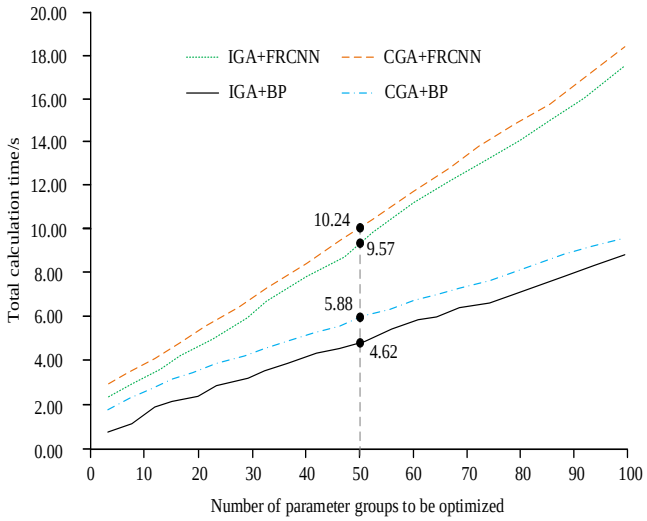

Fig. 7. Comparison of the computational efficiency of each optimization model.

In summary, the difference between the self-weight and maximum structural stress of the inspection vehicle designed in this study using neural networks instead of the finite element model output and the finite element model is less than 2%. In the engineering application environment of bridge inspection vehicles, this degree of error can be considered more accurate. The main reason for this situation is that neural networks have strong nonlinear relationship search and extraction capabilities, and there is indeed a complex nonlinear mapping relationship between the structural parameters of the bridge inspection vehicle and the corresponding structural self-weight and maximum stress. From the perspective of algorithm training speed, the IGA+BP model designed in this study has a slightly faster training speed than the comparison algorithm, because the BP neural network that makes up the algorithm itself is a three-layer structure, and the parameters to be optimized and the number of samples required for training are smaller than neural network algorithms such as Fast-RCNN. From the optimized parameter results, it can be seen that the optimal solution output by the design algorithm in this study corresponds to a significantly smaller self-weight than other algorithms, and the maximum stress and strain of the structure has not significantly increased compared to other methods, indicating that this method has certain application value in optimizing the structural parameters of bridge inspection vehicles.

V. Conclusion

In order to reduce the self-weight of the bridge inspection vehicle boom structure, this study designed an improved genetic algorithm and built an intelligent optimization model of the inspection vehicle boom structure by combining the BP neural network prediction model and the finite element model. The simulation experimental results show that the prediction value of the output of the test design variables from the prediction model constructed based on BP and Faster-RCNN neural network is less than 5% relative error to the calculation result of the finite element model, and can be used for the prediction model. The values of loss functions after convergence of the two models constructed using improved genetic algorithm, IGA+BP and IGA+FRCNN, are significantly lower than the other two models, and the former is higher than the latter with 1.52 and 3.15, respectively. Analysis of the optimal integer solutions of each optimized model reveals that the IGA+FRCNN model is the smallest in terms of maximum stress and maximum deformation, with 213.9 MPa and The maximum stress and maximum deformation of the IGA+FRCNN model are 213.9 MPa and 74.64 mm, respectively, followed by the IGA+B0P model with 219.50 MPa and 79.31 mm, respectively, which are lower than the allowable values of the material. From the perspective of measuring the total structural weight of the measuring arm, the IGA+B0P model has the lowest total structural weight of 4687.5 kg. Also the computation time of the model using the improved genetic algorithm is significantly lower than that of the model using the same prediction algorithm but without the improved genetic algorithm. When the number of groups with computational variables is 50, the computation time of CGA+BP, IGA+BP, CGA+FRCNN, IGA+ The computation time of each scheme is 5.88 s, 4.62 s, 10.24 s, and 9.57 s, respectively. It can be seen that the optimization model designed this time can obtain better self-weight optimization results of the bridge inspection vehicle arm structure quickly. However, the optimization effect of the model on other uncommon types of bridge inspection vehicles was not analyzed in the study, and this part will be added in the subsequent study.

References

[1] S. Z. Tang, M. J. Li, F. L. Wang, et al., "Fouling potential prediction and multi-objective optimization of a flue gas heat exchanger using neural networks and genetic algorithms," International Journal of Heat and Mass Transfer, vol. 152, no. 5, pp. 119488.1-119488.15, 2020.

[2] M. Xu, G. Zeng, D. Wu, et al., "Structural optimization of jet fish pump design based on a multi-objective genetic algorithm," Energies, vol. 15, no. 11, pp. 4104-4119, 2022.

[3] Y. Xue, Q. Zhang, F. Neri, "Self-adaptive particle swarm optimization-based echo state network for time series prediction," International Journal of Neural Systems, vol. 31, no. 12, pp. 579-584, 2021.

[4] D. J. Kozuch, F. H. Stillinger, P. G. Debenedetti, "Genetic algorithm approach for the optimization of protein antifreeze activity using molecular simulations," Journal of Chemical Theory and Computation, vol. 16, no. 12, pp. 7866-7873, 2020.

[5] K. Noh, J. H. Chang, "Joint optimization of deep neural network-based dereverberation and beamforming for sound event detection in multi-channel environments," Sensors, vol. 20, no. 7, pp. 1-13, 2020.

[6] J. Ren, H. Zhu, H. Wang, et al., "Multi-objective structural optimization of VL seal ring based on isight," Journal of Physics: Conference Series, vol. 1622, no. 1, pp. 012031.1-012031.6, 2020.

[7] R. Ghiasi, M. R. Ghasemi, "Feature selection in structural health monitoring big data using a meta-heuristic optimization algorithm," Journal of Computational Methods in Engineering, vol. 39, no. 1, pp. 1-27, 2020.

[8] M. Rabiei, A. J. Choobbasti, "Innovative piled raft foundations design using artificial neural network," Frontiers of Structural and Civil Engineering, vol. 14, no. 1, pp. 138-146, 2020.

[9] C. Millan-Paramo, J. Filho, "Exporting water wave optimization concepts to modified simulated annealing algorithm for size optimization of truss structures with natural frequency constraints," Engineering with Computers, vol. 37, no. 1, pp. 763-777, 2021.

[10] T. V. Varma, S. Sarkar, G. Mondal, "Buckling restrained sizing and shape optimization of truss structures," Journal of Structural Engineering, vol. 146, no. 5, pp. 4020048.1-4020048.12, 2020.

[11] B. Adil, C. Baykasolu, "Optimal design of truss structures using weighted superposition attraction algorithm," Engineering with Computers, vol. 36, no. 3, pp. 965-979, 2020.

[12] N. S. Usevitch, Z. M. Hammond, M. Schwager, "Locomotion of linear actuator robots through kinematic planning and nonlinear optimization," IEEE Transactions on Robotics, vol. 36, no. 5, pp. 1404-1421, 2020.

[13] T. Wang, X. Zhou, H. Zhang, "Control of forming process of truss structure based on cold metal transition technology," Rapid Prototyping Journal, vol. 28, no. 2, pp. 204-215, 2021.

[14] M. M. Kamiński, "On shannon entropy computations in selected plasticity problems," International Journal for Numerical Methods in Engineering, vol. 122, no. 18, pp. 5128-5143, 2021.

[15] X. Zhang, K. Hanahara, Y. Tada, Z. Pei, Z. Li, P. Sun, "Optimal design of a hanging truss with shape memory alloy wires," Transactions of the Canadian Society for Mechanical Engineering, vol. 44, no. 1, pp. 95-107, 2020.

[16] T. Nakamura, T. Yokaichiya, D. G. Fedorov, "Quantum-mechanical structure optimization of protein crystals and analysis of interactions in periodic systems," Journal of Physical Chemistry Letters, vol. 12, no. 36, pp. 8757-8762, 2021.

[17] C. Liu, C. Zhang, Y. Q. Cao, D. Wu, P. Wang, A. D. Li, "Optimization of oxygen vacancy concentration in HfO_2/HfO_x bilayer-structure ultrathin memristor by atomic layer deposition and its biological

synaptic behaviors," Journal of Materials Chemistry C, vol. 8, no. 36, pp. 12478-12484, 2020.

[18] E. Ching, J. Carstensen, "Truss topology optimization of timber-steel structures for reduced embodied carbon design," Engineering Structures, vol. 252, (Feb.1 Pt.2), pp. 113540.1-113540.11, 2022.

[19] V. Gasparetto, M. Elsayed, "Multiscale optimization of specific elastic properties and microscopic frequency band-gaps of architectured microtruss lattice materials," International Journal of Mechanical Sciences, vol. 197, no. 3, pp. 106320.1-106320.16, 2021.

[20] D. Wang, F. Shao, "Research of neural network structural optimization based on information entropy," Chinese Journal of Electronics, vol. 29, no. 4, pp. 632-638, 2020.

[21] D. Patel, D. Bielecki, R. Rai, et al., "Improving connectivity and accelerating multiscale topology optimization using deep neural network techniques," Structural and Multidisciplinary Optimization, vol. 65, no. 4, pp. 375-393, 2022.

[22] D. N. Kien, X. Zhuang, "A deep neural network-based algorithm for solving structural optimization," Journal of Zhejiang University-Science A, vol. 22, no. 8, pp. 609-620, 2021.

[23] Y. Li, "Multi-objective optimization design for battery pack of electric vehicle based on neural network of radial basis function (RBF)," Journal of Physics: Conference Series, vol. 1684, pp. 012156, 2020.

[24] Y. Fan, B. Feng, L. Yang, et al., "Application of artificial neural network optimization for resilient ceramic parts fabricated by direct ink writing," International Journal of Applied Ceramic Technology, vol. 17, no. 1, pp. 264-281, 2020.

[25] X. Han, Y. Kang, J. Sheng, et al., "Centrifugal pump impeller and volute shape optimization via combined NUMECA, genetic algorithm, and back propagation neural network," Structural and Multidisciplinary Optimization, vol. 61, no. 1, pp. 381-409, 2020.

[26] A. C. To, "Integrating geometric data into topology optimization via neural style transfer," Materials, vol. 14, no. 16, pp. 4551-4556, 2021.

[27] M. Baandrup, P. Noe Poulsen, J. Forbes Olesen, P. Henrik, "Optimization of truss girders in cable-supported bridges including stability," Journal of Bridge Engineering, vol. 25, no. 11, pp. 4020099.1-4020099.11, 2020.